OPTIMIZATION OF A SHELL-AND-TUBE DISTRICT HEAT CONDENSER FOR A SMALL BACK PRESSURE CHP PLANT

Jussi Saari*, Mariana M.O. Carvalho, Ekaterina Sermyagina, Esa Vakkilainen, Juha Kaikko.
*Author for correspondence
LUT School of Energy Systems,
Lappeenranta University of Technology,
Lappeenranta, 53850, Finland.
E-mail: saari@lut.fi

ABSTRACT

Wood-fired combined heat and power (CHP) plants are a proven technology for producing domestic, carbon-neutral heat and power in Nordic countries. Such plants are often of back-pressure configuration, the district heat condenser replacing the vacuum condenser of a condensing power plant. The condenser is usually a shell-and-tube heat exchanger with district heating water on the tube side. In this paper, a new approach is presented to optimize the condenser design considering not only the design-point performance, but also variations in the operating conditions. A power plant model is used to determine the plant performance (net power output and boiler fuel consumption) as a function of the main performance parameters of the condenser at each point. Cuckoo search algorithm is used for the optimization. The results show that although electricity price variation has a significant impact on plant net cash flow rate, the effects of electricity price and heat exchanger specific cost on condenser design are low.

INTRODUCTION

Bio-fired combined heat and power (CHP) plants have several advantages; they convert a carbon-neutral local energy source to heat and power at high efficiency. One challenge in the design and optimization of such plants is the variation of load: peak winter heat demand is typically an order of magnitude greater than minimum summer load. Currently the changes in the electricity markets in the Northern Europe also complicate CHP investment decisions: questions over renewable power subsidies and the future of nuclear power have created unusually high uncertainty over the future prices of electricity. This creates also challenges for plant and component design and optimization.

The focus of this paper is the optimization of a district heat (DH) condenser considering the annual net cash flow of the CHP plant as the objective function. DH condensers of CHP plants are typically U-tube shell-and-tube heat exchangers (STHX) with water on the tube side and steam condensing on the shell side.

The variation of heat load and operating conditions and their effect on both plant and condenser performance is considered using a multi-period model where the annual operating profile is approximated using four load points. A power plant model developed with the process simulation software IPSEpro is used to determine the plant performance (net power output and boiler fuel consumption) as a function of the condenser's conductance and condensate subcooling at each point. The performance results together with the heat exchanger cost model output are used to determine the objective function value. A range of electricity prices is considered to investigate the effect of the price on optimal condenser design.

Shell-and-tube heat exchanger optimization has been studied extensively, with several methods applied to cost and heat transfer modelling, and the optimization itself. Most studies model the heat exchanger cost as a function of the heat transfer area [1-10]. This approach has been shown to have drawbacks in general [11], and in condenser optimization in particular [12]. In this paper, the condenser manufacturing costs are divided into material cost and processing cost [11]. These were estimated by a combination of mechanical sizing methods presented in [11] to find the mass of each component, and a simplified version of processing cost model from [12] where only the most important processing costs are determined in detail.

The heat transfer modelling of a condenser presents certain challenges. An average overall heat transfer coefficient U is often adequate to determine the performance of a liquid-liquid STHX, but this approach would yield optimistic results for a low-pressure steam condenser with close temperature approach [13]. As a result, a multi-element 2D model treating the tube bundle as a network of heat exchangers, is used here [12, 13].

STHX design optimization is also made difficult by characteristics, such as several constraints, non-differentiability, possible multimodality, and a combination of discrete and continuous variables. Many optimization methods have been used in STHX optimization. Deterministic, non-iterative solutions for segmentally baffled single-phase STHX have been presented by several authors [1-3,5,14]. Most of these methods involve significantly simplified shell-side calculation, and are not suitable for multi-element calculation of condensing flows. Deterministic methods may also present converging issues, especially as the number of decision variables increases.

During the last 15 years, several stochastic optimization methods have been applied to heat exchanger optimization. These algorithms tend to be computationally heavy, but as CPU speeds increase, this becomes less of a limit in contrast to the robustness and ease of implementation in difficult optimization problems. Stochastic algorithms applied to STHX optimization include simulated annealing (SA) [15], particle swarm optimization (PSO) [8,10], and various evolutionary algorithms such as differential evolution (DE) [16], genetic algorithms (GA) [4,6,9,10,17], and harmony search (HS) [7]. In this study cuckoo search (CS), a relatively new and promising stochastic metaheuristic optimizer inspired by and loosely based on the brood-parasitic behaviour of cuckoo birds, was used. It's performance on a number of common benchmark functions has been shown to compare favourably to PSO and GA [18, 19].

NOMENCLATURE

a	[-]	Annuity factor for capital investment amortization
a_{nzl}	[m]	Major axis of the elliptic nozzle-to-shell joint
A	[m^2]	Area
c	[€/MWh]	Specific cost of energy or heat exchanger
	[€/m^2]	
c_p	[J/kgK]	Specific heat
C	[€/a]	Cost; Annual cash flow rate
d	[m]	Tube diameter
D	[m]	1. Diameter
f	[-]	Friction factor (Darcy)
g	[m/s^2]	Standard gravity
G	[W/K]	1. Conductivity
	[(kg/s)/m^2]	2. Mass velocity
	[-]	3. Generation of cuckoos
h	[W/m^{2}K]	Heat transfer coefficient (condensation or convection)
i	[-]	Interest rate
k	[W/mK]	Thermal conductivity
K	[m]	1. absolute surface roughness
	[-]	2. loss coefficient
k	[W/mK]	Thermal conductivity
L	[m]	Length
LHV	[MJ/kg]	Lower Heating value
$\dot{m}$	[kg/s]	Mass flow rate
n	[a]	Plant economic lifetime
NP	[-]	Number of parents in a cuckoo generation
NTU	[-]	Number of transfer units; NTU = UA/($\dot{m}\ c_p$)$_{min}$
Nu	[-]	Nusselt number
p	[Pa]	Pressure
P	[W],	1. Power
	[m]	2. Tube pitch
Pr	[-]	Prandtl number
$r_{O\&M}$	[-]	Ratio of operating and maintenance cost tot TCI
Re	[-]	Reynolds number
R_{tf}"	[m^{2}K/W]	Thermal fouling resistance
s	[mm],	1. Material thickness
	[-]	2. Step size vector
t	[h]	Time (in plant operation)
T	[°C]	Temperature
T_{furn}	[K]	Absolute temperature in boiler furnace
ΔT_{lm}	[°C]	Logarithmic mean temperature difference
TCI	[€]	Total Capital Investment
u	[-]	Uniform-distributed random variable
U	[W/m^{2}K]	Overall heat transfer coefficient
v	[-]	Uniform-distributed random variable
w	[m/s]	Velocity
x	[-]	Decision variable

Special characters

α	[-]	Scaling factor in optimization local search
β	[m]	Lévy exponent
ε	[-]	1. Heat exchanger effectiveness
	[-]	2. Uniformly distributed random variable
Φ	[W]	Thermal power
Γ	[-]	Gamma function,
μ	[Pa s]	Dynamic viscosity
ρ	[kg/m^3]	Density
σ	[N/mm^2]	Stress
σ^2	[N/mm^2]	Variance

Subscripts

bfl	Baffle (support) plate
c	Cold (water) side
CHP	Combined Heat and Power plant
D	Design point
DA	Deaerator
DH	District heat
eff	Effective
el	Electricity
f	Fuel
FG	Flue gas
FOB	Free on board
gr	Gravity
h	Hot (steam) side
HX	Heat exchanger
i	Element index in water flow direction
in	Inside; inlet
j	Element index in steam flow direction
L	Saturated liquid state
man	Manufacturing
mat	Material
max	Maximum
nzl	Nozzle
OD	Off-Design
OTL	Outer Tube Limit
out	Outside; outlet
pr	Processing
SC	Sub-cooling
SG	Steam generator
s	shell
sh	shear
tb	tube
V	Saturated vapour state

PROBLEM DEFINITION

A commercial small modular backpressure CHP plant with a 29 MW thermal output bubbling fluidized bed (BFB) boiler is considered [20]. At design point, the plant has a 20 MW DH output with 90/50 °C outlet/return temperatures. The turbine has a partial admission regulating stage and separate high-pressure (HP) and low-pressure (LP) parts with an extraction at the HP exhaust, controlled by the LP turbine inlet valve. The single backpressure DH condenser is not directly connected to turbine exhaust arrangement, but receives steam through a pipe. The design-point parameters are summarized in Table 1; schematic diagram is shown in Figure 1. The fuel is forest chips with 19.5 MJ/kg dry matter lower heating value (LHV), wet-basis moisture content varying from 55% (winter) to 40% (summer).

Table 1 Design-point parameters of the CHP plant model.

Parameter	Value
Power output; generator/net	8.66 / 8.00 MW
District heat (DH)	20.00 MW
Boiler thermal power	28.9 MW
Total (CHP) Efficiency	85 %
Steam parameters	90 bar / 500 °C

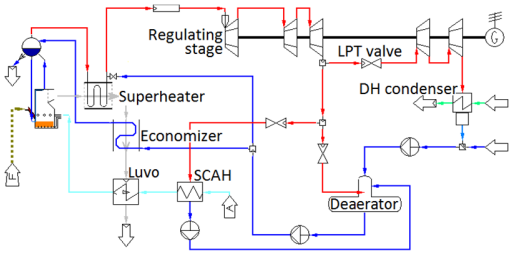

Figure 1 Schematic diagram of the CHP plant model.

The part-load modelling considers varying boiler and turbine performance. At off-design conditions (subscript OD), heat transfer rates Φ of those boiler surfaces where convection is the dominant heat transfer mode are calculated from design-point values (subscript D) assuming heat transfer to vary relative to 0.8:th power of flue gas mass flow rate $\dot{m}_{FG}$,

$$\Phi_{OD} = \Phi_D \left(\frac{\dot{m}_{FG,OD}}{\dot{m}_{FG,D}} \right)^{0.8} \frac{\Delta T_{lm,OD}}{\Delta T_{lm,D}}, \quad (1)$$

where ΔT_{lm} is the logarithmic mean temperature difference,

$$\Delta T_{lm} = \frac{(T_{h,in} - T_{c,out}) - (T_{h,out} - T_{c,in})}{\ln \frac{T_{h,in} - T_{c,out}}{T_{h,out} - T_{c,in}}}. \quad (2)$$

The steam generator heat transfer rate Φ_{SG} is estimated assuming an isothermal furnace where the heat transfer rate varies proportionally to the fourth power of absolute furnace temperature T_{furn},

$$\Phi_{SG,OD} = \Phi_{SG,D} \frac{T_{furn,OD}^4}{T_{furn,D}^4}. \quad (3)$$

Turbine pressure levels were determined using the ellipse law [21], and part-load efficiencies from polynomial curve fits based on [22] and [23]. The boundaries assumed for plant part-load operation are listed in Table 2.

Table 2 Off-design operating limits for the CHP plant.

Parameter	Design	min	max
Flue gas flow rate [kg/s]	17.27	-	19.5
Furnace temperature [°C]	904	700	950
Flue gas stack temperature [°C]	150	135	-
Turbine inlet steam flow rate [kg/s]	10.60	2.0	11.0
Deaerator pressure [bar]	5.6	3.0	8.0

Multi-period production model

A CHP plant is often sized for slightly over 50% of peak DH demand, resulting in 5000-7000 h annual operating time. Heat-only auxiliary boilers cover the peak consumption and demands below the CHP plant minimum load. The annual variation is approximated using a discretized model where each period is averaged to a single load point. The temperature levels of district heating water were set according to reference [24] based on the average ambient temperatures of each period. The ambient temperatures were estimated from Finnish Meteorological Institute monthly average temperature data in the central Finnish city of Jyväskylä. [25] The main parameters and the durations of the periods are listed in Table 3; Figure 2 shows the variation of heat and power production and fuel consumption.

Table 3 Average load points for the CHP plant.

Parameters	P1	P2	P3	P4
Period duration t [h]	1800	1400	1400	1400
Average ambient temperature [°C]	-8	0	+5	+10
DH water output/return T [°C]	90/55	80/50	75/45	75/45
DH power $\Phi_{DH,CHP}$ [MW]	20.0	18.0	14.0	10.0
Fuel: moisture [%] / LHV [MJ/kg]	55/7.4	50/8.5	50/8.5	45/9.6

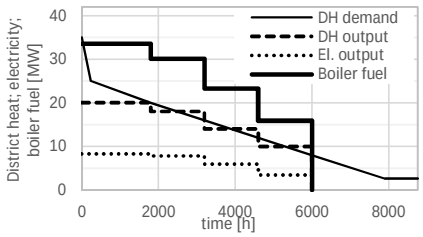

Figure 2 Annual CHP production and boiler consumption in the discretized multi-period model, and DH demand curve.

Condenser

A shell-and-tube U-tube condenser (Figure 3) in a round tube bundle and steam in pure cross flow was selected. Mechanical sizing was based on 250 °C design temperature and pressures of -1/+5 bar (shell) and -1/+16 bar (tubes). P235GH carbon steel was used for the tubes, P355GH for other parts. Yield strength of P355GH at 250 °C, σ_l = 210 N/mm^2, was used as the design stress in calculations. 60° tube pitch was used. Loss coefficients for pressure drop were set according to [26]. Inside and outside fouling resistances of $R"_{tf,in} = 8 \cdot 10^{-5}$ and $R"_{tf,out} = 1 \cdot 10^{-5}$ m^{2}K/W were assumed. The values were set lower than figures in TEMA standards [27], which were considered to represent pessimistic rather than typical figures.

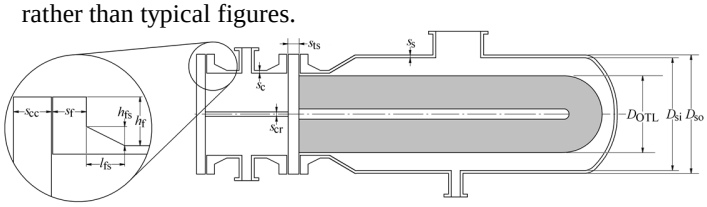

Figure 3 District heat condenser construction.

Objective function

The objective function to maximize is the annual net cash flow of the CHP plant, obtained from

$$C_{tot} = \sum_{P=1}^{4} t_P \left(P_{el} c_{el} + \Phi_{DH} c_{DH} - \Phi_f c_f \right) - a TCI_{tot} - r_{O\&M} TCI_{tot}, \quad (4)$$

where a is the amortization factor for the total capital investment (TCI) at interest rate i and economic lifetime n. Table 4 lists these and other economic parameter values. The cost the CHP plant excluding the condenser was estimated TCI_{CHP} = 26·10^6 € [28]. The DH condenser cost TCI_{DHC} was obtained by setting the cost of installed equipment as 3.3 times the FOB cost (C_{FOB}) [29]. The C_{FOB} was obtained from manufacturing cost C_{man} using a mark-up estimate consisting of 30% overhead cost, 5% contingency and 10% manufacturer's profit.

Table 4 Values of economic parameters.

Parameter	value
Maximum annual operating time t [h]	6000
Interest rate i [-]	0.10
Plant economic lifetime n [a]	20
Annual O&M cost ratio $r_{O\&M,}$ [%]	0.04
Wood chip price c_f [€/MWh$_{LHV}$]	20
District heat price c_{DH} [€/MWh]	60

The manufacturing cost C_{man} consists of material cost C_{mat} and processing cost C_{pr}, where C_{mat} is clearly the dominant factor. Following material costs were assumed: tubesheet 3.5 €/kg; shell, channel and flanges 2.5 €/kg; and baffles 2.0 €/kg. Tube cost was set as a function of diameter based on a curve fit made on data available from commercial suppliers. Tube length was unlimited, but a 10% cost penalty was applied on tubes longer than 20 m before bending to U-tubes. Nozzle sizes were assumed unaffected by other dimensions and not considered.

Shell and channel are sized against internal pressure and buckling at -1 bar vacuum according to [31], and the tubesheet based on the simpler method of the older standard [26]. Flange dimensions were estimated from curve fits for standard flange sizes for heat exchangers as function of shell diameter.

Of the processing cost, baffle-related costs are the largest one [11] and any attempt to minimize the baffle costs will also significantly impact the heat transfer surface geometry. Baffle processing costs were thus modelled in detail according to the methodology of [11], while other processing costs were estimated at 10% of C_{mat} based on the results presented in [11].

The CHP plant fuel consumption Φ_f and heat and power production Φ_{DH} and P_{el} at each load points are functions of condenser performance: effective conductance $G_{eff} = U_{eff}A$, and condensate sub-cooling ΔT_{SC}. The effective conductance is defined as

$$G_{eff} = \Phi_{DH}\left(\ln\frac{T_{h,in} - T_{DH,out}}{T_{h,in} - T_{DH,return}}\right)/\left(T_{DH,return} - T_{DH,out}\right), \qquad (5)$$

where $T_{h,in}$ is the saturation temperature at the shell nozzle, $T_{sat}(p_{nzl})$. This is different from $G = UA$ based on an average of local U values, since local heat transfer rate in the bundle is also affected by varying vapour pressure, and hence $T_{sat}(p)$. It is the G_{eff} that determines the terminal temperature difference TTD, turbine exhaust pressure and thereby the effect on the CHP plant power production and boiler fuel consumption.

Sub-cooling may result from thick liquid inundation layer on the tubes, ineffective gas venting, or steam pressure drop. In a compact low-cost condenser design steam velocity may become high, the resulting pressure drop reducing $T_{sat}(p)$. This will manifest itself as sub-cooling as well as reduced G_{eff}. Subcooling due to thick inundation layers is unlikely in a small condenser considered here, and effective gas venting does not pose significant cost variations or restrictions to the design; these effects are thus not considered.

In the objective function evaluation the effects of G_{eff} and ΔT_{SC} on plant performance were determined using polynomial curve fits based on data generated with the plant model. A very good agreement of R^2=1.00 was obtained for $P_{el} = f(G_{eff})$ and $\Phi_f = f(G_{eff})$, and acceptable ($R^2 > 0.9$) also for ΔT_{SC} effect. The ΔT_{SC} proved to have relatively small impact on both P_{el} and Φ_f: <0.2 % per each 1 °C of sub-cooling.

The point P1 represents the boiler-limited maximum load. As the boiler load is at maximum during P1, increasing condenser G_{eff} increases power production at the expense of DH output. Since the Φ_{DH} production thus varies from the nominal value of 20 MW (Table 1), the period lengths of P1 and P2 are adjusted to prevent mean Φ_{DH} from exceeding the DH load curve.

The decision variables of the optimization are listed in Table 5. The straight length x_3 considers only effective heat transfer area; tube length covered by baffles or tube sheet is not part of this variable, but is factored in the condenser mass and cost calculation.

Table 5 Decision variables x and their initialization ranges.

x	Definition	Initialization range
x_1	Ratio of shell to bundle $D_{sh,in}/D_{OTL}$	$0.5 < x_1 < 0.95$
x_2	Number of tube passes	$x_2 \in \{2,4\}$
x_3	Straight tube length per pass L_{str} [m]	$3.0 < x_3 < 12.0$
x_4	Tube outside diameter d_o [mm]	$x_4 \in \{10, 12, 14, 16, 18, 20, 22, 25, 28, 30\}$
x_5	Tube pitch/ diameter ratio P/d_o	$1.25 < x_5 < 1.50$
x_6	Water free-flow area $A_{fr,c}$ [m^2]	$0.2 < x_6 < 1.0$

Constraints are listed in Table 6. Maximum tube-side velocity was set at the maximum water velocity in carbon steel tubes according to reference [30]. Maximum shell-side velocity, defined as the maximum velocity at the tightest spacing between the tubes, was set at the upper end of the recommended range for vapours at approximately atmospheric pressure in reference [29].

Table 6 Constraints.

Variable	Constraint	Variable	Constraint
Tube-side velocity	$w_c \leq$ 3.0 m/s	Shell-side velocity	$w_h \leq 30$ m/s
Tube pitch	$P \geq 1.25 d_o$	Tubesheet ligament	$(P - d_o) \geq 5$ mm
Condenser length	$L_{HX} \leq 15.0$ m	Condenser diameter	$D_{HX} \leq 3.5$ m

The optimization algorithm produces candidate solutions represented as vectors **x** of six design variable values. The outline of the algorithm to evaluate the objective function value for such a candidate vector is shown in Figure 4. The step of finding the district heat rate Φ_{DH} and adjusting the steam pressure until convergence is described in detail in the following chapter.

HEAT TRANSFER MODEL

The model determines iteratively the performance of the condenser at different load points by assuming a steam pressure p_h, solving the heat transfer rate given the water flow rate and return temperature, and correcting the pressure until DH production and water outlet temperature match the DH load.

The heat transfer calculation is based on reference [13]. Each U-tube of 2 passes pass is split in i_{max} slices in tube direction, and j_{max} circular segments in steam flow direction. A 180° U-element, i_U = ½(i_{max}-1)+1, joins the two passes. Flows entering element (i,j) are set by outlet conditions of (i-1,j) and (i,j-1). Constant T_{sat} and heat transfer coefficients are assumed in each element.

The flows are calculated iteratively in water flow direction from i=1 to i_{max} using equations (6) to (11). Each slice i is also calculated iteratively, starting with an estimated steam flow to (i,1), and continuing until no vapour flow exits from (i,j_{max}).

$$U_{i,j} = \left[\left(d_o/d_i\right)\left(R''_{tf,in} + h_{c,i,j}^{-1}\right) + R''_w + h_{h,i,j}^{-1} + R''_{tf,in}\right]^{-1} \qquad (6)$$

$$NTU_{i,j} = \frac{U_{i,j}A_{i,j}}{\dot{m}_{c,j}c_{p,c,i,j}} \qquad (7)$$

$$\varepsilon_{i,j} = 1 - e^{-NTU_{i,j}} \qquad (8)$$

$$\Phi_{i,j} = \varepsilon_{i,j}\dot{m}_{c,j}c_{p,c,i,j}\left(T_{h,i,j} - T_{c,i,j}\right) \qquad (9)$$

$$T_{c,i+1,j} = T_{c,i,j} + \frac{\Phi_{i,j}}{\dot{m}_{c,j}c_{p,c,i,j}} \qquad (10)$$

$$\dot{m}_{h,V,i,j+1} = \frac{\dot{m}_{h,V,i,j}h_{h,V,i,j} + \dot{m}_{h,L,i,j}h_{h,L,i,j} - \dot{m}_{h,V,i,1}h_{h,L,i,j+1} - \Phi_{i,j}}{h_{h,V,i,j+1} - h_{h,L,i,j+1}} \qquad (11)$$

The tube inside heat transfer coefficient h_c is based on the Petukhov-Popov correlation [32], the friction factor f obtained from the iterative Colebrook-White equation:

$$Nu_c = \frac{h_{c,i,j}d_i}{k_c} = \frac{0.125 f \cdot Re_c Pr_c}{1.07 + \frac{900}{Re_c} - \frac{0.62}{1+10Pr_c} + 12.7\sqrt{\frac{Pr_c^{2/3}f}{2} - 1}}\left(\frac{\mu}{\mu_c}\right)^{0.14}, \qquad (12)$$

$$\frac{1}{\sqrt{f}}' = -2\log_{10}\left[\frac{2.51}{Re_c\sqrt{f}} + \frac{K/d_i}{3.71}\right]. \qquad (13)$$

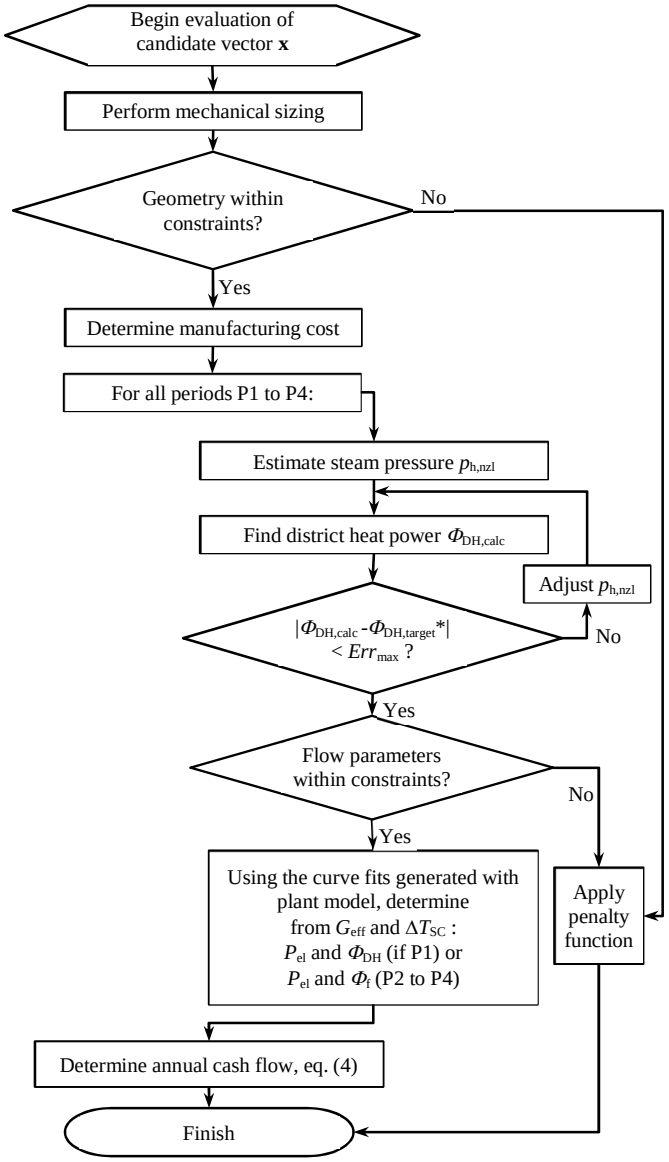

* In period P1 $\Phi_{DH,target}$ is adjusted during the iterative heat transfer calculation to a value that with the latest value of G_{eff} and ΔT_{SC} will yield a boiler fuel rate matching the boiler maximum continuous rating, thus making the variable Φ_f a de facto constant. For periods P2 to P4, $\Phi_{DH,target}$ is the Φ_{DH} listed in Table 3.

Figure 4 Flow chart for objective function evaluation.

Water pressure drop Δp_c was obtained from

$$\Delta p_c = \frac{\rho_c w_c^2}{2}\left(f\frac{L_{tb}}{d_i} + K_{nzl,c,in} + \frac{N_{tbp}}{2}\left(K_{tb,in} + K_U + K_{tb,out}\right) + K_{nzl,c,out}\right), \quad (14)$$

The condensation heat transfer coefficient at j:th segment $h_h(j)$ is obtained approximating the net effect of gravity- and shear-dominated coefficients $h_{h,gr}$ and $h_{h,sh}$ with an averaging formula (16) and an inundation correction (17):

$$Nu_{h,gr} = \frac{h_{h,gr} d_o'}{k_l} = 0.728\left[\frac{\rho_L(\rho_L - \rho_V) g h_{fg} d_o^3}{\mu_L k_L \Delta T}\right]^{1/4} \text{ [33]}, \quad (15)$$

$$Nu_{h,sh} = \frac{h_{h,sh} d_o'}{k_l} = 0.59\sqrt{\frac{w_V d_o \rho_L}{\mu_L}} \text{ [34]}, \quad (16)$$

$$h_h = \sqrt{0.5h_{h,sh}^2 + \sqrt{0.25h_{h,sh}^4 + h_{h,gr}^4}} \text{ [35]}, \quad (17)$$

$$h_h(j) = h_h\left[\left(j \cdot N_{Lj}\right)^{5/6} - \left(j \cdot N_{Lj} - 1\right)^{5/6}\right] \text{ [35]}, \quad (18)$$

where N_{Lj} is the average number of tube rows in steam flow direction per each segment j.

Steam pressure drop takes place at the nozzle (Δp_{nzl}) and tube bundle. Δp_{nzl} was calculated assuming half a velocity head lost at velocities at nozzle, 90° turn from the nozzle, and the free area between the bundle and shell in shell axis direction,

$$\Delta p_{nzl} = 0.5\frac{\rho_{V,nzl}\dot{V}_{V,nzl}^2}{2A_{nzl}^2} + 0.5\frac{\rho_{V,90°}\dot{V}_{V,90°}^2}{2A_{90°}^2} + 0.5\frac{\rho_{V,ann}\dot{V}_{V,s,ax}^2}{2A_{s,ax}^2}; \quad (19)$$

$$A_{nzl} = \frac{\pi D_{nzl}^2}{4};$$

$$A_{90°} = P_{nzl} \cdot \left[\tfrac{1}{2}\left(D_{s,in} - D_{OTL}\right) - h_{ip}\right];$$

$$A_{s,ax} = 2 \cdot \left(\frac{\pi D_{s,in}^2}{4} - A_{bfl}\right)$$

where P_{nzl} is the perimeter of an ellipse with major axis of a_{nzl} and minor axis of D_{nzl} obtained using Ramanujan's approximation formula [36], D_{bfl} is the diameter of the circular part of a baffle plate, h_{ip} is the height of the impingement plate from the tube bundle, and A_{bfl} is the area covered by the support plates in tube axis direction, shown as gray in Figure 5 below.

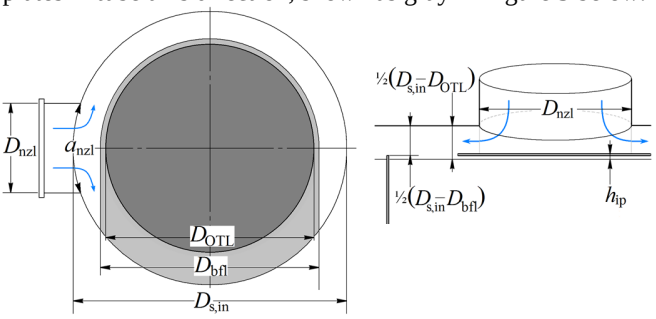

(a) (b)

Figure 5 Geometry at steam entry to the shell.

The pressure drop in the tube bundle was determined using Jakob correlation based on vapour mass velocity at the smallest area between the tubes G_{max}:

$$\Delta p_h = \frac{2\left[0.25 + 0.1175\left(P/d_o\right)^{-1.08}\right]\left(w_{V,max} d_o \rho_V \mu_V\right)^{-0.16} G_{max}^2}{\rho_V}. \text{ [37]} \quad (20)$$

OPTIMIZATION ALGORITHM: CUCKOO SEARCH

First introduced in 2009, the Cuckoo Search (CS) is one of the most recent metaheuristic optimization algorithms. Like many metaheuristics, such as evolutionary algorithms, wasp, ant, and bee colony algorithms, and bat algorithm, it is inspired by processes observed in nature: in this case, the well-known brood parasitic behaviour of many cuckoo species [38], as well as a search pattern known as Lévy flights [38] which maximises the efficiency of resource search [39] and has been observed in many mobile foraging species [38, 39].

Like many nature-inspired metaheuristics, the CS also operates not with a single point that it tries to improve, but a population of candidate solutions, which in CS represent cuckoo

eggs. Each cuckoo lays one egg to one nest per generation. As this number is fixed, there is no practical distinction to be made between a cuckoo, an egg, and a nest.

Each iteration begins with an attempt at global search by a so-called Lévy flight, a random walk where step length is drawn from Lévy probability distribution resulting in clusters of short steps connected by rare longer leaps. From each cuckoo i of generation G a new candidate solution is generated for generation G+1. The new candidate, which replaces the old one if it yields an objective function value better than the original, is obtained from

$$x_i^{G+1} = x_i^G + \alpha \cdot \Delta x_{best} \cdot s \cdot n, \quad (21)$$

where α is a scaling factor, vector Δx_{best} is the difference between current vector x_i^G and the so far best solution x_{best}, $\Delta x_{\text{best}} = x_{\text{best}}^G - x_i^G$, s is a Lévy-distributed step size vector and n is a vector of random variables with a standard normal distribution. All vectors have a size of D. The step size vector s is obtained with Mantegna's algorithm originally published in [40] as cited in [18] using two normal-distributed random variable vectors u and v of size D and a Lévy exponent β:

$$s = u \cdot v^{-1/\beta}, \quad (22)$$

where all elements of u and v have a mean of zero, and variances of 1 (v) and σ^2 (u), respectively. σ^2 is calculated from

$$\sigma^2 = \left[\frac{\Gamma(1+\beta)}{\beta \cdot \Gamma(\tfrac{1}{2}+\tfrac{1}{2}\beta)} \cdot \frac{\sin(\tfrac{1}{2}\pi\beta)}{2^{\frac{1}{2}(1+\beta)}} \right]^{1/\beta}, \quad (23)$$

where Γ is the gamma function, $\Gamma(n) = (n\text{-}1)!$. The second step is exploitative local search by replacing each element d of every egg (candidate vector) i at probability p_a, representing the detection of cuckoo eggs by the host bird. Each new decision variable d in a new candidate vector is obtained from

$$x_{i,d}^{G+1} = x_{i,d}^G + \alpha \cdot r \cdot H \cdot (p_a - \varepsilon) \cdot (x_{j,d}^G - x_{k,d}^G), \quad (24)$$

where H means the Heaviside function, α is the scaling factor as used in eq. (17), and r and ε are uniformly distributed random variables. Vectors x_j and are x_k are chosen randomly from the population. Again, the new candidate vector produced with eq. (20) replaces the previous solution – either the original x_i^G, or if the Lévy flight succeeded, the result of eq. (17) – if the new candidate vector yields a better objective function value.

The CS algorithm has proven to be relatively insensitive to the values of α and β; the values of 0.01 and 1.5, which can be used with most problems [18], were used in this study. A switching probability p_a = 0.25, population size of NP = 60 cuckoos, and stopping condition of 300 generations were used.

RESULTS

Optimization was performed with electricity price range of 40-80 €/MWh. While the low-end scenarios for future electricity prices in Nordic countries include even lower prices, unsubsidized bio-CHP production is unlikely to be profitable in these scenarios. Three cases of heat exchanger cost were considered: base, -20% optimistic and +20% pessimistic. The main parameters corresponding to 40, 60 and 80 €/MWh electricity price and base case of condenser price are listed in Table 7.

The condenser optimized for 40 €/MWh electricity price is far smaller than the other two, which are similar. While the smaller exchanger is much cheaper, the shorter design increases the relative share of shell, channel and tube sheet, which results in almost 50% greater specific cost of heat transfer area.

Table 7 Condensers optimized for different electricity prices, base case manufacturing cost assumed.

P_{el} [€/MWh$_{el}$]	40	60	80
$x_1=D_{OTL}/D_s$	0.737	0.750	0.740
$x_2=N_{tbp}$	2	2	2
$x_3=L_{str}$	4.000	8.054	8.066
$x_4=d_o$ [mm]	18.0	16.0	16.0
$x_5=P/d_o$ [-]	1.278	1.313	1.313
$x_6=A_{fr,c}$ [m^2]	0.045	0.079	0.086
L_{tot} [m]	4.982	9.345	9.386
D_{tot} [m]	0.821	1.096	1.148
D_{ch} [m]	0.677	0.898	0.926
D_s [m]	0.821	1.064	1.134
L_s [m]	4.376	8.543	8.557
s_{ts} [mm]	92	116	121
s_{chc} [mm]	34	43	45
m_{tot} [kg]	3 633	10 760	11 515
$N_{tb/pass}$ [-]	255	599	645
A_{tot} [m^2]	120	497	536
C_{tot} [10^6 €], eq.(1)	0.08	0.82	1.58
C_{FOB} [10^3 €]	37	107	114
c_{FOB} [€/m^2]	307	216	213

When the parameters used for plant performance estimation, G_{eff} and ΔT_{SC}, are plotted over the range of electricity price c_{el} for all condenser cost cases (Figure 6), a clear step change at approximately 50 €/MWh$_{el}$ becomes evident. At c_{el} values above the step change, G_{eff} varies from 1350 to 1550 kW/K and subcooling remains stable at ΔT_{SC} = 0.6±0.5 °C; below, the ranges vary from 400 to 600 kW/K and 0.2 to 0.4 °C. Above the step change, condenser manufacturing cost case has < 5% impact on optimal conductance and heat transfer area at any given c_{el}.

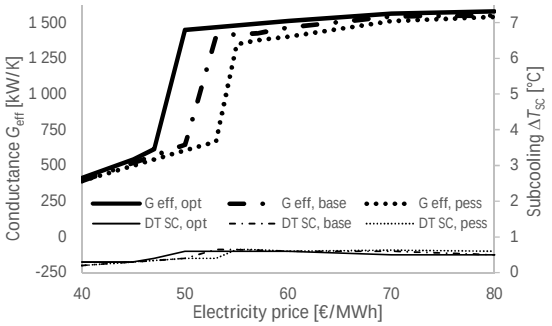

Figure 6 Conductance (thick line) and subcooling (thin) in optimized condensers at varying electricity price and optimistic (-20%), baseline and pessimistic (+20%) cost assumption.

It is evident that although a large step change takes place in condenser size and cost, the design optimized for an electricity price immediately below the step change price level does not yet represent the minimum condenser size within the constraints; conductances continue to reduce towards the lower electricity prices. The CHP plant also remains profitable with a positive net cash flow even assuming an expected return rate of 10% for the investment, and in fact no similar step change in net cash flow rate takes place (Figure 7). It appears that the step change

represents the point at which increasing the DH production during period P1 at the expense of power generation starts to outweigh the benefit that could be achieved by increased power output at part load.

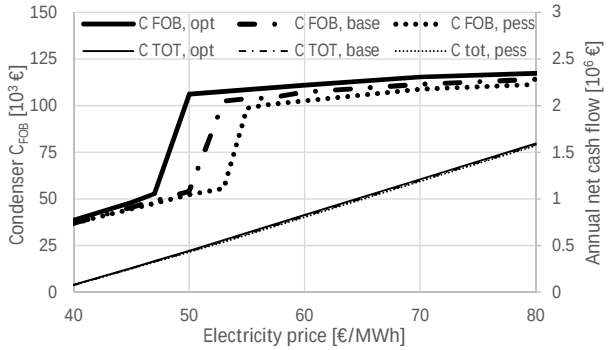

Figure 7 Condenser FOB cost and plant annual net cash flow as function of electricity price.

Figure 8 presents the optimal values of maximum-load (period P1) TTD and water pressure drop Δp_c as a function of electricity price above the step change. The optimum values fall within a relatively narrow range at all electricity prices and condenser cost scenarios; mostly 2-3 °C TTD and 0.4-0.5 bar Δp_c. TTD becomes smaller at a reducing rate towards increasing electricity prices as could be expected, while the Δp_c curves tip downwards at the high end of electricity prices in all cases. The tip downwards in Δp_c could be an indication of the role of the pumping power becoming relatively more important as the cost of obtaining more power output from the turbine increases with what is already a relatively large, low-TTD condenser design.

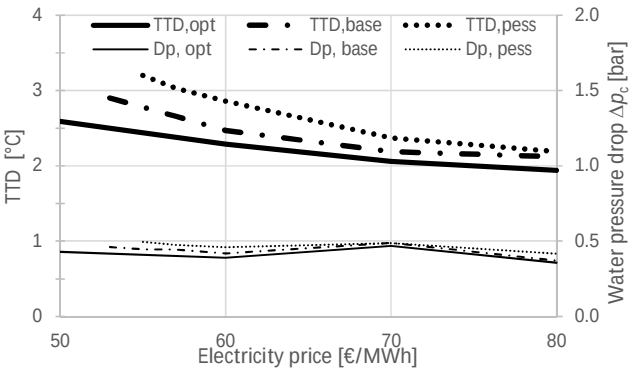

Figure 8 Condenser terminal temperature difference and water-side pressure drop at maximum load (load point P1).

CONCLUSIONS

Shell-and-tube district heat back pressure condenser optimization for a small modular power plant was studied using a multi-period model to account for annual variation of load and operating conditions. Cuckoo search algorithm was used in the optimization. A cost model incorporating elements from both Caputo et al. [11] and Saari et al. [12] was implemented to evaluate equipment cost.

The methods used were successful for the problem, and the resulting condenser configurations appear mostly typical for such equipment. While convergence proof for a stochastic metaheuristic is not possible, the curve shapes resulting from running the algorithm at gradually changing parameter values are relatively smooth with some notable but systematic exceptions, indicating reliable performance.

A steep step change occurs at approximately electricity price of 50 €/MWh_{el}. Above the step change price, the main finding was that while net cash flow rate for the investment is significantly affected by varying electricity price, variations in either electricity price or condenser cost have only little impact on what is the optimal design for the condenser.

For lower electricity price ranges the optimized designs were much smaller in size and cheaper in cost. Although the CHP plant remained profitable with a positive net cash flow rate down to the lowest electricity price considered, 40 €/MWh, the optimization result that appeared to maximize DH production at the expense of power output casts some doubt over the preferability of a CHP plant over a heat-only boiler at such conditions.

The possibility of altering the conductance by varying condensate level in the condenser shell was not considered here. A design where condensate level could be allowed to raise in the tube bundle to submerge some of the heat transfer tubes would allow a given condenser design both deliver high conductance and thus maximum electricity output at part load, and reduce the power output for increased DH production during the full-load period. This would likely be the best strategy in a situation when electricity price is less than district heat price, but still sufficiently high that the CHP plant is remains profitable.

REFERENCES

[1] F. Jegede and G. Polley, "Optimum heat exchanger design: process design", *Chemical Engineering Research & Design*, vol. 70, pp. 133-141, 1992.

[2] F. T. Mizutani, F. L. Pessoa, E. M. Queiroz, S. Hauan and I. E. Grossmann, "Mathematical programming model for heat-exchanger network synthesis including detailed heat-exchanger designs. 1. Shell-and-tube heat-exchanger design", *Ind Eng Chem Res*, vol. 42, pp. 4009-4018, 2003.

[3] K. Muralikrishna and U. Shenoy, "Heat exchanger design targets for minimum area and cost", *Chem. Eng. Res. Design*, vol. 78, pp. 161-167, 2000.

[4] R. Selbaş, Ö Kızılkan and M. Reppich, "A new design approach for shell-and-tube heat exchangers using genetic algorithms from economic point of view", *Chemical Engineering and Processing: Process Intensification*, vol. 45, pp. 268-275, 2006.

[5] M. Serna and A. Jiménez, "A compact formulation of the Bell–Delaware method for heat exchanger design and optimization", *Chem. Eng. Res. Design*, vol. 83, pp. 539-550, 2005.

[6] J. M. Ponce-Ortega, M. Serna-González and A. Jiménez-Gutiérrez, "Use of genetic algorithms for the optimal design of shell-and-tube heat exchangers", *Appl. Therm. Eng.*, vol. 29, pp. 203-209, 2009.

[7] M. Fesanghary, E. Damangir and I. Soleimani, "Design optimization of shell and tube heat exchangers using global sensitivity analysis and harmony search algorithm",

Appl. Therm. Eng., vol. 29, pp. 1026-1031, 2009.
[8] V. Patel and R. Rao, "Design optimization of shell-and-tube heat exchanger using particle swarm optimization technique", *Appl. Therm. Eng.*, vol. 30, pp. 1417-1425, 2010.
[9] S. Sanaye and H. Hajabdollahi, "Multi-objective optimization of shell and tube heat exchangers," *Appl. Therm. Eng.*, vol. 30, pp. 1937-1945, 2010.
[10] H. Hajabdollahi, P. Ahmadi and I. Dincer, "Thermoeconomic optimization of a shell and tube condenser using both genetic algorithm and particle swarm," *Int. J. Refrig.*, vol. 34, pp. 1066-1076, 2011.
[11] A. C. Caputo, P. M. Pelagagge and P. Salini, "Manufacturing cost model for heat exchangers optimization", *Appl. Therm. Eng.*, vol. 94, pp. 513-533, 2016.
[12] J. Saari, S. Afanasyeva, E. K. Vakkilainen and J. Kaikko, "Heat transfer model and optimization of a shell□and□tube district heat condenser," in *Proceedings of International Conference on Efficiency, Cost, Optimization, Simulation and Environmental Impact of Energy Systems (ECOS) 2014*, Turku, 2014, pp. 1920-1933.
[13] J. Saari, J. Kaikko, E. Vakkilainen and S. Savolainen, "Comparison of power plant steam condenser heat transfer models for on-line condition monitoring," *Appl. Therm. Eng.*, vol. 62, pp. 37-47, 2014.
[14] A. L. Costa and E. M. Queiroz, "Design optimization of shell-and-tube heat exchangers", *Appl. Therm. Eng.*, vol. 28, pp. 1798-1805, 2008.
[15] P. D. Chaudhuri, U. M. Diwekar and J. S. Logsdon, "An automated approach for the optimal design of heat exchangers", *Ind Eng Chem Res*, vol. 36, pp. 3685-3693, 1997.
[16] B. Babu and S. Munawar, "Differential evolution strategies for optimal design of shell-and-tube heat exchangers", *Chemical Engineering Science*, vol. 62, pp. 3720-3739, 2007.
[17] S. Sanaye and M. Dehghandokht, "Modeling and multi-objective optimization of parallel flow condenser using evolutionary algorithm", *Appl. Energy*, vol. 88, pp. 1568-1577, 2011.
[18] X. Yang and S. Deb, "Cuckoo search: recent advances and applications," *Neural Computing and Applications*, vol. 24, pp. 169-174, 2014.
[19] X. Yang, "Cuckoo search and firefly algorithm: Overview and analysis," in *Cuckoo Search and Firefly Algorithm* Anonymous Springer, 2014, pp. 1-26.
[20] S. Komulainen, "Voimalaitoksen käytönaikaisen optimoinnin määrittely", (In Finnish; Eng. Definition of power plant on-line optimization) [master's thesis]. Lappeenranta, Finland: Lappeenranta University of Technology, 2012.
[21] W. Traupel, *Thermische Turbomaschinen: Thermodynamisch-Strömungstechnische Berechnung.* Springer-Verlag, 1966.
[22] T. Tveit, T. Savola and C. Fogelholm, "Modelling of steam turbines for mixed integer nonlinear programming (MINLP) in design and off-design conditions of CHP plants", in *Proceedings of the 46th Conference on Simulation and Modeling (SIMS 2005)*, 2005, pp. 13-14.
[23] M. Jüdes, S. Vigerske and G. Tsatsaronis, "Optimization of the design and partial-load operation of power plants using mixed-integer nonlinear programming," in *Optimization in the Energy Industry*, Springer, 2009, pp. 193-220.
[24] L. Koskelainen, R. Saarela, K. Sipilä. *Kaukolämmön käsikirja*. (In Finnish; eng. "Handbook of district heating"). Energiateollisuus ry (Association of Finnish Energy Industry), 2006.
[25] P. Pirinen, H. Simola, J. Aalto, J. P. Kaukoranta, P. Karlsson, R. Ruuhela. *Tilastoja Suomen ilmastosta 1981-2010*. (In Finnish; eng."Statistics about the climate of Finland 1981-2010"). Finnish Meteorological Institute, 2012.
[26] SFS-Käsikirja 13, "Paineastiat. Mitoitus" (In Finnish; Eng. Pressure vessels. Dimensioning), 1996.
[27] Tubular Exchanger Manufacturers Association, Inc., "Standards of the Tubular Exchanger Manufacturers Association, 9th Edition", 2007.
[28] T. Kuitunen, "Uusiutuvista energialähteistä tuotetun sähkön tukijärjestelmät Euroopan unionissa ja niiden vaikutus biomassavoimalaitosten kannattavuuteen" (In Finnish; Eng. Subsidy systems for electricity produced from renewable sources in the European Union and their effect on the profitability of biomass power plants) [master's thesis]. Lappeenranta, Finland: Lappeenranta University of Technology, 2011.
[29] R. Sinnott, *Coulson & Richardson's Chemical Engineering Design*. Oxford, UK: Butterworth-Heinemann, 2005.
[30] J. Taborek, "3.3 Shell-and-tube heat exchangers / 3.3.5 Input data and recommended practices", *Heat Exchanger Design Handbook 3: Thermal and Hydraulic Design of Heat Exchangers"*. Hemisphere Publishing Corporation, United States of America, 1983.
[31] SFS-EN 13445-3, "Lämmittämättömät painesäiliöt" (In Finnish; Eng. Unfired pressure vessels). 2002.
[32] R. K. Shah and D. P. Sekulic, *Fundamentals of Heat Exchanger Design*. John Wiley & Sons, 2003.
[33] W. Nusselt, Die Oberflachenkondensation des Wasserdampfes. (In German; Eng. Film condensation of water vapour). *Z. Vereines Deutsch. Ing.* Vol. 60, pp. 541-546,569-575, 1916.
[34] I.G. Shekriladze, V.I. Gomelauri, Theoretical study of laminar film condensation of flowing vapour, *International Journal of Heat and Mass Transfer*, Vol. 9, pp. 581–591, 1966.
[35] S. Kakac, *Boilers, Evaporators and Condensers*. Wiley & Sons, 1991.
[36] L. Råde, B. Westergren, *Mathematics Handbook for Science and Engineering.* Studentlitterature, Sweden, 1995.
[37] J.P. Holman, *Heat Transfer*. McGraw-Hill Book Company, Singapore, 1989.
[38] X.Yang, *Nature-inspired optimization algorithms*, Elsevier, 2014.
[39] S. Focardi, P. Montanaro, E. Pecchioli, "Adaptive Lévy Walks in Foraging Fallow Deer", *PLoS ONE* 4(8):e6587, 2009
[40] R. N. Mantegna, "Fast, accurate algorithm for numerical simulation of Levy stable stochastic processes," *Physical Review E*, vol. 49, pp. 4677, 1994.